Solid State Phenomena Vols. 205-206 (2014) pp 34-39

doi:10.4028/www.scientific.net/SSP.205-206.34

Precipitation of interstitial iron in multicrystalline silicon

AnYao Liu[1, a] and Daniel Macdonald[1, b]

[1]Research School of Engineering, Australian National University, Canberra, ACT, 0200, Australia

[a]anyao.liu@anu.edu.au (corresponding author), [b]daniel.macdonald@anu.edu.au

Keywords: iron, multicrystalline silicon, precipitation, supersaturation, spatial distribution

Abstract The internal gettering of iron in silicon via iron precipitation at low processing temperatures is known to improve solar cell efficiencies. Studies have found that the optimal temperature lies in the range of 500°C-600°C. In this paper, we present experimental results on quantitatively analysing the precipitation of interstitial Fe in multicrystalline silicon wafers during the 500°C-600°C thermal annealing processes. The concentration and the spatial distribution of interstitial Fe in mc-Si were measured by the photoluminescence imaging technique. It was found that, apart from the processing temperature, the Fe precipitation time constant is highly dependent on the supersaturation ratio and the density and types of the precipitation sites.

Introduction

Iron is a common efficiency-limiting impurity in silicon for solar cells. Internal gettering of iron, by a low temperature annealing process, has been shown to be effective in reducing the interstitial iron concentrations and thus improve the minority carrier lifetimes in both mono- and multi- crystalline silicon materials [1-4]. These studies [1-4] have found that the optimal annealing temperature lies in the range of 500°C-600°C, where the Fe point defects have sufficiently high diffusivity to move to the precipitation sites and the Fe solubility is low enough to cause precipitation to occur. In multicrystalline silicon (mc-Si), the precipitation sites are mainly the structural defects within the material. In this study, we will experimentally examine the precipitation mechanisms of interstitial Fe in mc-Si wafers with respect to temperature and time, in the range of 500°C-600°C, both near the grain boundaries (GBs) and within the grains. Photoluminescence imaging is employed to produce high resolution images of the interstitial Fe concentrations [5, 6], which allows us to study the changes in the concentration and the distribution of interstitial Fe (Fe_i) across mc-Si wafers after temperature processes at 500°C-600°C.

Experimental methods

The mc-Si wafers used in this study were from near the bottom of a commercially-grown boron-doped directionally-solidified ingot. The resistivity of the wafers is $1.4\Omega cm$. The wafers were $330\mu m$ thick, and $125mm \times 125mm$ in size. The two wafers were labelled 1 and 2, and were sawn into smaller pieces labelled a-d, where the letters represents its lateral position in the mc-Si wafer. The wafers were chemically etched, cleaned, and then annealed in oxygen at 1000°C to grow silicon oxide layers for surface passivation. Oxide passivation was chosen as it remains stable during the subsequent annealing steps, unlike silicon nitride passivation, for example. Annealing at 1000°C also uniformly distributes the interstitial Fe concentrations across the wafers, as shown in the Fe image in Fig. 1. Dissolution of precipitated Fe is expected during such high temperature processes [7], however, our previous study [8] into the neighbouring wafers has found that the amount of dissolution is not significant compared to the initial as-cut interstitial Fe concentration ($[Fe_i]$) on the order of $10^{12} - 10^{13}$ cm^{-3}. The wafers were grouped into two sets and were annealed at either 500°C or 600°C for various time intervals ranging from minutes to hours, with accumulated time durations of 10-15 hours. The ambient gas during the low temperature annealing was a mixture of 95% Argon and 5% Hydrogen, which we have found maintains the surface passivation. The interstitial Fe concentrations were measured after each thermal annealing step, by using photoluminescence imaging for spatially resolved Fe_i concentration distributions [6]. The derivation of the Fe_i

concentration is based on the well-established method of measuring the minority carrier lifetimes before and after the dissociation of the Fe-B pairs in silicon, via strong illumination in this experiment. A magnifying lens was used, giving an image pixel size of around 23 micrometers. A point spread function [9] was applied to deconvolve image smearing caused by the lateral photon scattering within the Si-CCD camera. The average interstitial Fe concentrations of Wafer 1 and Wafer 2, after oxidation and prior to any low temperature annealing, were $3\times10^{12} - 3.5\times10^{12}$ cm^{-3} and $9\times10^{12} - 1.1\times10^{13}$ cm^{-3} respectively.

Results and Discussion

Average [Fe_i] across a wafer. The interstitial Fe concentrations demonstrate a clear reduction trend as the annealing time accumulates. An example is shown in Fig. 2, which illustrates the results of two wafers annealed at 600°C and were of different initial Fe_i concentrations. We can see that, firstly, the reductions in the interstitial Fe concentrations are approximately exponential. Secondly, the two wafers demonstrate different reduction time constants. The time constant is determined via an exponential decay fit to the data. The reduction in the interstitial Fe concentration is interpreted as the increase in the amount of precipitated Fe. The [Fe_i] reduction time constants, that is, the Fe precipitation time constants, for all wafers are listed in Table 1. The saturation ratio is calculated as the ratio between the [Fe_i] of the wafer and the Fe solubility [10] at the anneal temperature. As the [Fe_i] in the wafer decreases with annealing time, the saturation ratio decreases accordingly.

Table 1 Summary of the precipitation time constants and saturation ratios across mc-Si wafers

500°C			600°C			
Wafer label	**Precipitation time constant, τ (minutes)**	**Saturation ratio**	**Wafer label**	**Precipitation time constant, τ (minutes)**	**Saturation ratio**	**Initial [Fe_i] (cm^{-3})**
1-a	360	1480 - 230	1-c	350	63-11	3×10^{12} – 3.5×10^{12}
1-b	330	1270 - 170	1-d	370	64-17	
2-a	230	4660 - 180	2-c	140	171-14	9×10^{12} – 1.1×10^{13}
2-b	280	4190 - 270	2-d	150	215-12	

For wafers that underwent the same temperature annealing, but with different initial [Fe_i], the precipitation time constants decrease as the saturation ratios increase. This suggests that the degree of supersaturation has a significant impact on the Fe precipitation, consistent with Refs [1, 2]. The results show that the effect of supersaturation is less prominent when the saturation ratio is above 1000 (500°C annealing), as compared to ratios of around 100 (600°C annealing).

Comparing the precipitation time constants of Wafer 2 pieces, which had similar initial [Fe_i] but were annealed at different temperatures, the results show that the ones annealed at 600°C have smaller time constants than those annealed at 500°C. This is as expected, as the diffusivity of Fe_i increases with temperature, meaning that the Fe_i atoms could move faster to the structural defects to precipitate at higher temperatures (if other precipitation-permitting factors are present). However, the precipitation time constants of Wafer 1 pieces show no distinguishable difference between the 500°C and the 600°C anneals. This is owing to the low degree of saturation ratios experienced by the wafers during the 600°C anneals, which hinders precipitation at the structural defects, and counteracts the effect of the increased diffusivity. Supersaturation is therefore a necessary driving force for the Fe precipitation.

Krain *et al* [4] reported a precipitation time constant of 18 minutes for mc-Si wafers annealed at 500°C, measured by the Quasi-Steady-State-Photoconductance (QSSPC) technique across the wafers. This is much smaller than our results (Table 1). The Fe_i saturation ratios in their study are in fact smaller than ours, and hence the effect of supersaturation cannot explain the discrepancy. The likely explanation lies in the possible differences in the density and the types of the precipitation sites of the tested mc-Si wafers. This is discussed in the following section.

Lateral changes in [Fe_i] distribution. Figs. 1 and 3 show the interstitial Fe images of the same wafer before and after annealing at 500°C for an extended cumulative time. It is clear from Fig. 3 that the reduction in [Fe_i] is not uniform across a mc-Si wafer after annealing. Fig. 4 shows the linescans of the Fe_i concentrations across one grain boundary (GB1 marked in Fig. 3), before and after annealing at 500°C for various cumulative time durations. The linescans were fitted with an iron diffusion model [11], which allows an estimation of the diffusion length of Fe atoms during annealing, and the precipitation velocity at the GB. The diffusion lengths of the Fe atoms derived from the model agree well with those calculated from the known annealing temperature and time, as shown in Fig. 5. This means that the precipitation of Fe at GB1 is diffusion limited at 500°C.

The amount of Fe gettered by the grain boundaries during each annealing step could be determined from the reduction in the [Fe_i] in the denuded zones, as represented by the shaded area in between two linescans shown in Fig. 4. The cumulative amount of Fe precipitation can then be calculated and plotted as a function of the cumulative annealing time, as shown in Fig. 6 for GB1. An exponential relation of $C(t) = C_o[1-\exp(-t/\tau)]$ is used to fit the data. For GB1, the fitting parameter of C_o is 1.3×10^{13} cm^{-3}, which is very close to the initial [Fe_i] in vicinity of the GB prior to any low temperature anneals. From this fit, the precipitation time constant of GB1 was found to be around 250 minutes.

The precipitation time constants of the intra-grain regions are shown in Fig. 7, which is a plot of the average Fe_i concentrations of the intra-grain regions (denoted in Fig. 3) with respect to the annealing time. The four regions demonstrate very different precipitation time constants, ranging from 150 to 670 minutes. This is most likely due to variations between the grains in terms of the density, and possibly the type, of precipitation sites present. Therefore it is perhaps more meaningful to analyse the precipitation mechanism for each type of the precipitation site, as the average precipitation time constant derived for one mc-Si wafer is not applicable for other mc-Si samples.

Summary

In this paper, we present experimental results on quantitatively analysing the precipitation of interstitial Fe in mc-Si wafers during the 500°C-600°C thermal annealing processes. A significant reduction of the interstitial Fe concentrations was observed after annealing in this temperature range. The [Fe_i] reduction time constant, that is, the Fe precipitation time constant, is found to depend on the process temperature, supersaturation ratio, and density and type of precipitation sites. A high degree of supersaturation is identified as a necessary driving force for Fe precipitation. The Fe precipitation time constant varies significantly across a mc-Si wafer. In our future work, the Fe precipitation mechanism will be examined for different types of structural defects in mc-Si materials.

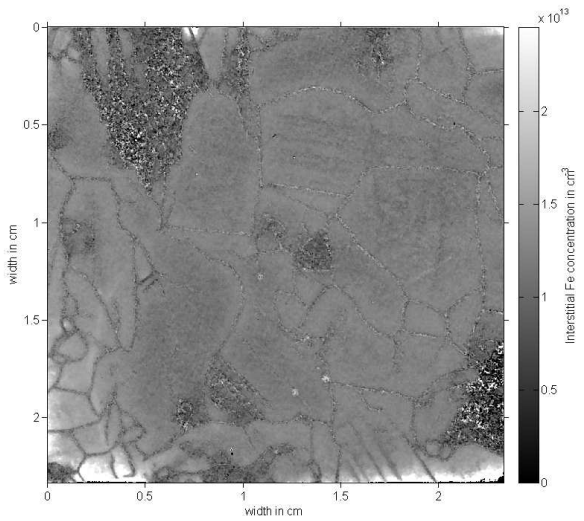

Fig. 1. [Fe_i] image of Wafer 2-b, after annealing at 1000°C in oxygen for surface passivation, and prior to any low temperature anneals.

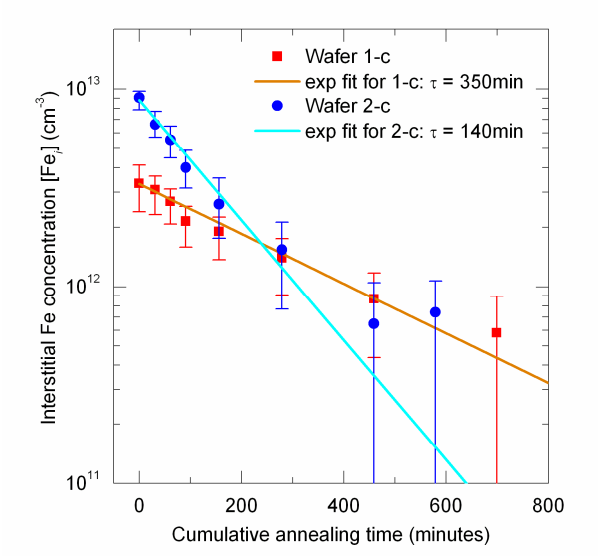

Fig. 2. Average [Fe_i] as a function of the cumulative annealing time for wafers annealed at 600°C.

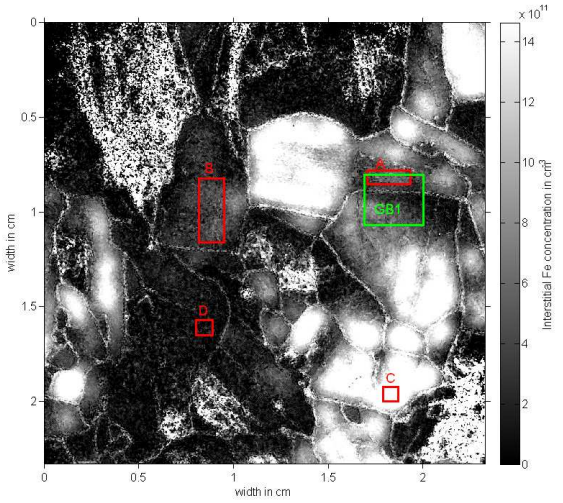

Fig. 3. [Fe_i] image of Wafer 2-b, after subsequent annealing at 500°C for a cumulative time duration of 867 minutes.

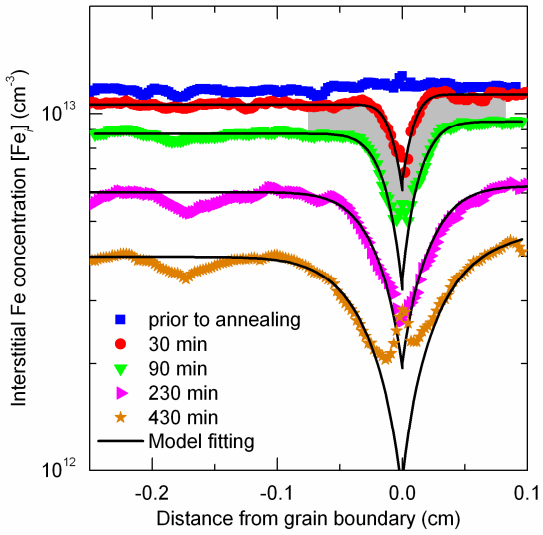

Fig. 4. Linescans of the [Fe_i] images across the GB1 denoted in Fig. 3, before and after anneals at 500°C for different cumulative time durations. The solid lines are model fitting [11] to the experimental data. The area shaded in grey represents the amount of Fe gettered by the GB during the annealing process occurred in between the red and green data.

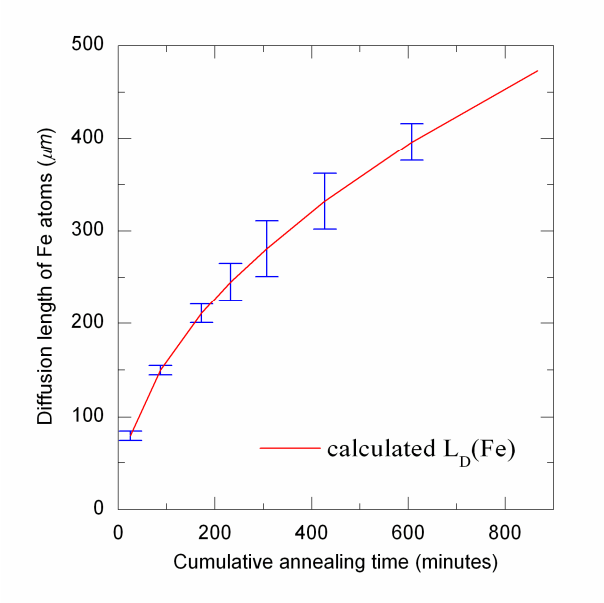

Fig. 5. Diffusion length of Fe atoms, estimated via model fitting [11] the [Fe_i] linescans of GB1 (Figs. 3 and 4), as a function of the annealing time. The solid line is the calculated diffusion length of Fe based on the known annealing temperature and time.

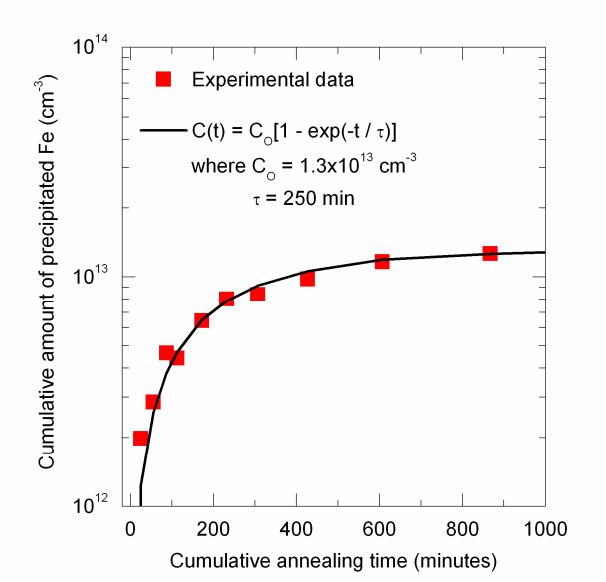

Fig. 6. Cumulative concentration of precipitated Fe as a function of the annealing time for the grain boundary GB1 denoted in Fig. 3.

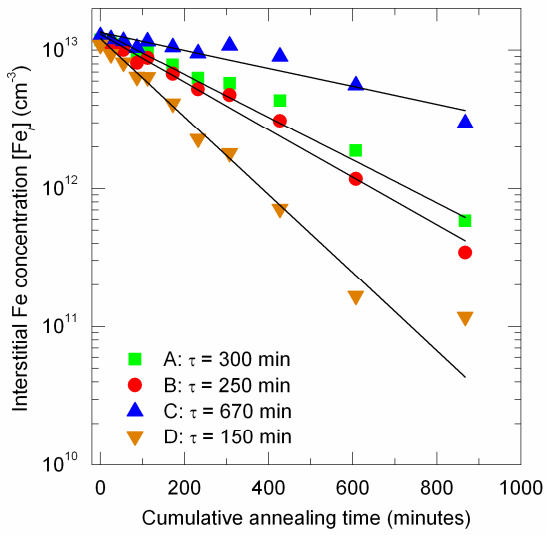

Fig. 7. Comparison of the changes in the Fe_i concentrations of Wafer 2-b's intra-grain regions (denoted in Fig. 3).

References

[1] W. B. Henley and D. A. Ramappa, Iron precipitation in float zone grown silicon, Journal of Applied Physics, 82 (1997) 589-594.

[2] A. Haarahiltunen, H. Väinölä, O. Anttila, M. Yli-Koski, and J. Sinkkonen, Experimental and theoretical study of heterogeneous iron precipitation in silicon, Journal of Applied Physics, 101 (2007) 043507.

[3] M. D. Pickett and T. Buonassisi, Iron point defect reduction in multicrystalline silicon solar cells, Applied Physics Letters, 92 (2008) 122103.

[4] R. Krain, S. Herlufsen, and J. Schmidt, Internal gettering of iron in multicrystalline silicon at low temperature, Applied Physics Letters, 93 (2008) 152108.

[5] T. Trupke, R. A. Bardos, M. C. Schubert, and W. Warta, Photoluminescence imaging of silicon wafers, Applied Physics Letters, 89 (2006) 044107.

[6] D. Macdonald, J. Tan, and T. Trupke, Imaging interstitial iron concentrations in boron-doped crystalline silicon using photoluminescence, Journal of Applied Physics, 103 (2008) 073710.

[7] T. Buonassisi, A. A. Istratov, S. Peters, C. Ballif, J. Isenberg, S. Riepe, W. Warta, R. Schindler, G. Willeke, Z. Cai, B. Lai, and E. R. Weber, Impact of metal silicide precipitate dissolution during rapid thermal processing of multicrystalline silicon solar cells, Applied Physics Letters, 87 (2005) 121918.

[8] A. Y. Liu, D. Walter, and D. Macdonald, Studying precipitation and dissolution of iron in multicrystalline silicon wafers during annealing, in The 22nd International Photovoltaic Science and Engineering Conference Hang Zhou, China, 2012.

[9] D. Walter, A. Y. Liu, E. Franklin, D. Macdonald, B. Mitchell, and T. Trupke, Contrast enhancement of luminescence images via point-spread deconvolution, in Photovoltaic Specialists Conference (PVSC), 2012 38th IEEE, 2012, 000307-000312.

[10] J. D. Murphy and R. J. Falster, Contamination of silicon by iron at temperatures below 800°C, Physica Status Solidi RRL, 5 (2011) 370-372.

[11] A. Y. Liu, D. Walter, S. P. Phang, and D. Macdonald, Investigating Internal Gettering of Iron at Grain Boundaries in Multicrystalline Silicon via Photoluminescence Imaging, IEEE Journal of Photovoltaics, 2 (2012) 479-484.